Ball Balancing Robot: construction, modeling and control design

Flávio H. B. Lima
Dept. of Telecomm. and Control Eng.
Escola Politécnica da USP
São Paulo, Brazil
flavio.henrique.lima@usp.br

Eduardo Poleze
Dept. of Telecomm. and Control Eng.
Escola Politécnica da USP
São Paulo, Brazil
eduardo.poleze@usp.br

Gabriel P. das Neves
Dept. of Telecomm. and Control Eng.
Escola Politécnica da USP
São Paulo, Brazil
gabriel.pereira.neves@usp.br

Bruno A. Angélico
Dept. of Telecomm. and Control Eng.
Escola Politécnica da USP
São Paulo, Brazil
angelico@lac.usp.br

***Abstract*—Ball Balancing Robots (BBRs) are a class of robots capable to balance themselves over a sphere. With the right modeling and planning of trajectories, they can move towards every direction in the horizontal plane of movement. This work gathers construction aspects, modeling and design of a stabilizing controller. Modeling a BBR is a complex work, since they are often under-actuated systems and the actuators are not aligned with the coordinates system, making necessary torques and velocities transformations. Practical results are presented in order to validate the modeling and control design.**

***Index Terms*—Optimal Control, Feedback stabilization, Robot dynamics, Mobile robots.**

I. Introduction

Ball-Balancing Robots (BBRs) are robots that balance on a sphere. There are basically two distinct forms of construction. In the first, there are two quadrature wheels positioned around the equator of the sphere, together with a third support wheel, as presented in [1]. In the second form, there is a set of omni-directional wheels equally spaced in contact with the ball, which allows movement in all directions of the horizontal plane, as shown in [2]. The latter has a more complicated model, since the relationships between torques and speeds produced by the wheel and the torques and velocities that balance the body are not trivial, as seen in Section III.

The study of this class of self-balanced robots is interesting, since theoretically they can move in any direction of the horizontal plane, without changing orientation, unlike two-wheeled self-balancing robots (ex *Segway*), which need to change the orientation for a change of direction, [3], [4]. Recently, in [5], it was proposed a vehicle with three omni-directional wheels acting on a ball, and four control moment gyroscope for balancing, transferring, and rotating. This is the first BBR-type people-carrying robot.

This work presents the constructive aspects of a BBR developed with three omni-directional wheels driven by DC gear-motors. Some aspects of mechanical modeling and the design of a Quadratic Linear Regulator (LQR) in discrete time are also presented.

The authors would like to thank the Fundação de Amparo à Pesquisa do Estado de São Paulo (FAPESP) for the grant 2017/22130-4.

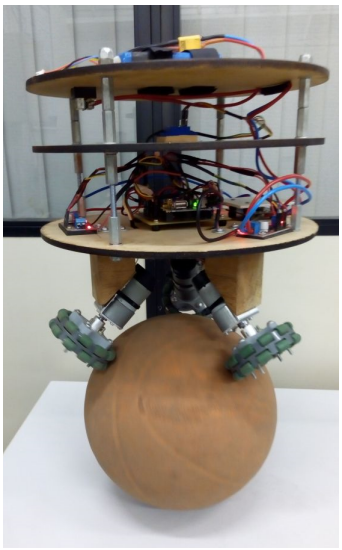

Fig. 1. Developed BBR.

II. Robot Construction

The robot was designed in a 3D CAD Software, from where most of the parameters presented in Table I were obtained. The robot was built with three 6mm MDF (Medium-Density Fiberboard) plates to allocate all its electronic and mechanical components. In addition, a basketball of size 7 was used. The final prototype is shown in Fig. 1.

Three DC gear-motors with encoders were used, whose parameters are also shown in Table I, were coupled under the body at an angle $\psi = 50°$ with respect to the vertical axis. They were separated by 120°. In addition to the motors, three omni-directional wheels were used.

A Teensy 3.2 microcontroller was used to embed the control algorithm, with a sampling frequency $f_s = 100$ [Hz]. An IMU GY-87 was considered to measure angular positions and velocities of the body. The angular velocities of the body were obtained directly from the measurements of the gyroscope, but the angular positions were obtained by fusing the gyroscope with the accelerometer by means of a Kalman

TABLE I
PHYSICAL PARAMETERS

Variable	Description	Value
M_b	Ball mass	0.6 [kg]
J_b	Moment of inertia of the ball	5.68×10^{-3} [kg m^2]
R_b	Ball radius	0.118 [m]
R_w	Wheel radius	0.1179 [m]
M_c	Body mass	2.7579 [Kg]
J_r	Moment of inertia of the body in x	0.03368376 [kg m^2]
J_p	Moment of inertia of the body in y	0.03382657 [kg m^2]
J_y	Moment of inertia of the body in z	0.02249327 [kg m^2]
J_w	Moment of inertia of the wheel	45.88×10^{-6} [kg m^2]
d	Distance to centers of mass	0.24380132 [m]
K_t	Motor torque constant	0.118 [Nm/A]
K_e	Motor speed constant	0.229 [V s/rad]
R_m	Motor armature resistance	2.4 [Ω]

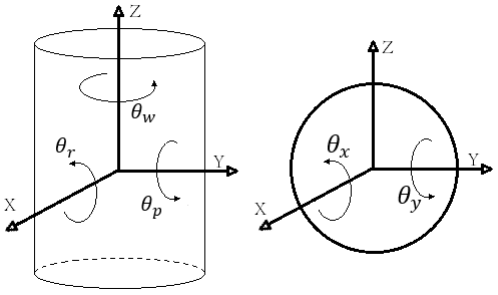

Fig. 2. Angles that describe the movements of the ball and the robot's body.

filter. Omni-directional wheel speeds were estimated using the Backward (Euler) method with a low pass filter of the incremental position measurement from the encoders. Three H-bridge drivers, model VNH2SP30, were also employed.

III. SYSTEM MODELING

The modeling procedure was based on the work presented in [6], for balance of an unicycle with reaction wheel. The nonlinear model does not include precession and Coriolis effects, since the velocities used to calculate kinetic energy are obtained directly from the absolute position vectors.

Defining θ_x and θ_y as the rotation angles of the ball around the axes x and y, respectively, and θ_p, θ_r and θ_w the rotation angles of the robot around the axes y (*pitch*), x (*roll*) and z (*yaw*), respectively, it is possible to define the generalized variables vector as

$$q = \begin{bmatrix}\theta_x & \theta_y & \theta_p & \theta_r & \theta_w\end{bmatrix}^\top. \tag{1}$$

The degrees of freedom of the robot can be described by this set of variables. They are represented in Fig. 2.

It is assumed that the reference coordinate system is fixed on the ground. With this, it is possible to describe the center of mass (CM) position of the ball p_b, and the relative position p_r between the CMs, as can be seen in Fig. 3.

Being R_b the radius of the ball, its position can be described by

$$p_b = \begin{bmatrix}R_b\theta_y & R_b\theta_x & R_b\end{bmatrix}^\top. \tag{2}$$

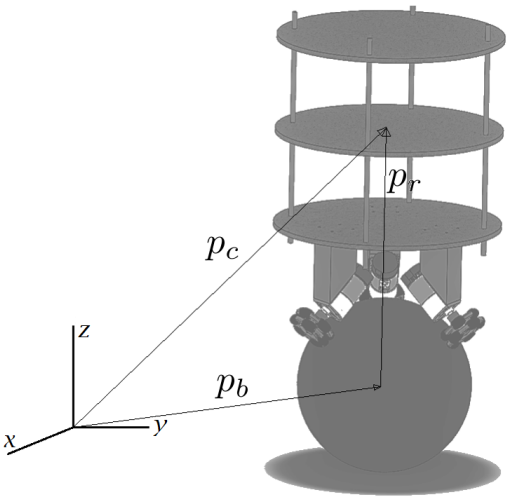

Fig. 3. Robot position vectors described with a single coordinate system.

It is assumed that the wheels of the robot are always in contact with the ball. In this way, the distance between the CMs is constant and equal to d. Thus, p_r is determined by

$$p_r = \begin{bmatrix} d\sin(\theta_p) \\ -d\cos(\theta_p)\sin(\theta_r) \\ d\cos(\theta_p)\cos(\theta_r)\end{bmatrix}. \tag{3}$$

Therefore, the CM position of the body, p_c, can be described by

$$p_c = p_b + p_r. \tag{4}$$

The linear velocities are calculated from the derivative of the position vectors, such that

$$v_b = \begin{bmatrix}R_b\dot{\theta}_y & R_b\dot{\theta}_x & 0\end{bmatrix}^\top, \tag{5}$$

and

$$v_c = \begin{bmatrix} R_b\dot{\theta}_y + d\,\mathrm{c}(\theta_p)\dot{\theta}_p \\ -R_b\dot{\theta}_x - d\,\mathrm{c}(\theta_p)\,\mathrm{c}(\theta_r)\dot{\theta}_r - d\,\mathrm{s}(\theta_p)\,\mathrm{s}(\theta_r)\dot{\theta}_p \\ -d\,\mathrm{c}(\theta_p)\,\mathrm{s}(\theta_r)\dot{\theta}_r - d\,\mathrm{s}(\theta_p)\,\mathrm{c}(\theta_r)\dot{\theta}_p\end{bmatrix}, \tag{6}$$

where $\mathrm{c}(\theta)$ and $\mathrm{s}(\theta)$ is a notation to express $\cos(\theta)$ and $\sin(\theta)$, respectively.

The angular velocities of the ball (ω_b) and the body (ω_b) are directly derived from the generalized variables, as expressed in

$$\omega_b = \begin{bmatrix}\dot{\theta}_x & \dot{\theta}_y & 0\end{bmatrix}^\top \tag{7}$$

and in

$$\omega_c = \begin{bmatrix}\dot{\theta}_r & \dot{\theta}_p & \dot{\theta}_w\end{bmatrix}^\top. \tag{8}$$

In order to calculate the system Lagrangian given by

$$L(q,\dot{q}) = \sum K(q,\dot{q}) - \sum U(q), \tag{9}$$

it is necessary to compute the potential energies (U) and kinetic (K) of each part of the robot.

Considering m_b as the mass of the ball, I_b its inertia tensor, defined as $\mathrm{diag}(J_b, J_b, J_b)$, and g the acceleration of gravity, the kinetic K_b and potential U_b energies of the ball are expressed by

$$K_b = \frac{1}{2}m_b v_b^T v_b + \frac{1}{2}\omega_b^T I_b \omega_b, \tag{10}$$

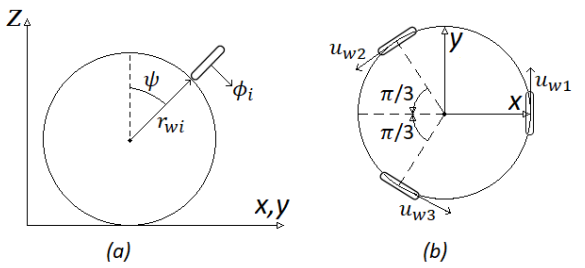

Fig. 4. Geometric aspects to describe the speeds of the omni-directional wheels (Adapted from: van der Blonk, 2014 , [7]).

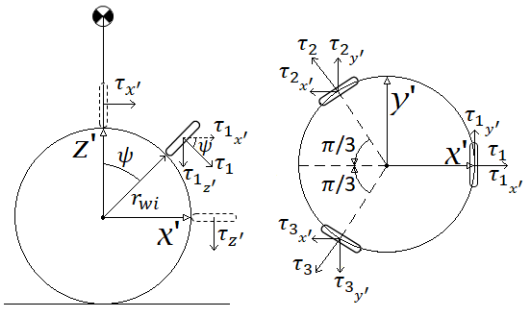

Fig. 5. Geometric transformation of virtual torques to motor torques (Adapted from: van der Blonk, 2014, [7]).

and

$$U_b = m_b g R_b. \tag{11}$$

Likewise, by considering m_c as the mass of the body and I_c as its inertia tensor in the form $\mathrm{diag}(J_r, J_p, J_y)$, its kinetic and potential energies, K_c and U_c, are calculated by

$$K_c = \frac{1}{2} m_c v_c^T v_c + \frac{1}{2} \omega_c^T I_c \omega_c \tag{12}$$

and

$$U_c = m_c g [R_b + d\cos(\theta_p)\cos(\theta_r)]. \tag{13}$$

The potential energy of the wheels is considered in (13). Thus, by considering J_w as the moment of inertia of the omni-directional wheel around its rotational axis, and $\dot{\phi}_i$ the angular velocity of the i-th wheel, the kinetic energy associated with the wheels is given by

$$K_w = \sum_{i=1}^{3} \frac{1}{2} \dot{\phi}_i^T J_w \dot{\phi}_i. \tag{14}$$

Assuming no slippage occurs between the omni-directional wheels and the ball, the speed of the wheels can be geometrically related to the speeds of the ball. The geometric aspects of the problem can be seen in Fig. 4. r_{wi} represents the vector defined between the center of the ball and the point of contact of the i-th wheel with the ball. u_{wi} represents the versor that points to the same direction as the linear velocity of the i-th wheel, at the point of contact with the ball.

Knowing the radius r_w of the omni-directional wheels, the angular velocity of each one can be described by

$$\dot{\phi}_i = \frac{1}{r_w} (\omega_b \times r_{wi})\, u_{wi}\,, \quad i = 1, 2, 3. \tag{15}$$

With the equations (10) to (14), the Lagrangian (9) can be determined. Being $\tau_{\mathrm{ext},i}$ the external torque related to the generalized variable q_i, the Euler-Lagrange equations can be calculated with

$$\frac{d}{dt}\left(\frac{\delta L}{\delta \dot{q}_i}\right) - \frac{\delta L}{\delta q_i} = \tau_{\mathrm{ext},i}. \tag{16}$$

The external torques that act in the body have the same modulus and opposite directions to the torques that act on the ball. Thus, the external torques can be described by three virtual torques: τ_x, τ_y and τ_z, such that

$$\tau_{\mathrm{ext}} = \begin{bmatrix} -\tau_x & -\tau_y & \tau_y & \tau_x & \tau_z \end{bmatrix}^\top. \tag{17}$$

The motors do not act directly on the axes of the virtual torques used in (17), so a geometric transformation of the torques was applied, as can be observed in Fig. 5.

Let τ_i be the i-th motor torque and $\{x'y'z'\}$ a coordinate system positioned in the center of the ball. z' is defined as the axis that connects the CMs of the ball and the body , and τ_1 is positioned in the $x'z'$ plane.

When the robot is in equilibrium, the systems $\{xyz\}$ and $\{x'y'z'\}$ are aligned. The relation between the virtual torques and the torques of the motors is given by

$$\begin{bmatrix} \tau_x \\ \tau_y \\ \tau_z \end{bmatrix} = \begin{bmatrix} \cos(\psi) & \frac{-\cos(\psi)}{2} & \frac{-\cos(\psi)}{2} \\ 0 & \frac{\sqrt{3}\cos(\psi)}{2} & \frac{-\sqrt{3}\cos(\psi)}{2} \\ \sin(\psi) & \sin(\psi) & \sin(\psi) \end{bmatrix} \begin{bmatrix} \tau_1 \\ \tau_2 \\ \tau_3 \end{bmatrix}. \tag{18}$$

Let τ_i, PWM_i and $\dot{\phi}_i$ be the torque, the PWM duty cycle and the angular velocity associated with the i-th motor, respectively, and $V_{\max}$ the maximum input voltage. Hence, the DC motor equations are described by

$$\tau_i = \frac{K_t (V_{\max} PWM_i - K_e \dot{\phi}_i)}{R_m}. \tag{19}$$

In order to find a linearized model that could express the dynamics of the system in a linear state space representation, the following vector was defined

$$x = \begin{bmatrix} \dot{\theta}_x & \dot{\theta}_y & \theta_p & \dot{\theta}_p & \theta_r & \dot{\theta}_r & \dot{\theta}_w \end{bmatrix}^\top \tag{20}$$

as the state vectors. The system inputs are defined as

$$u = \begin{bmatrix} PWM_1 & PWM_2 & PWM_3 \end{bmatrix}^\top. \tag{21}$$

The system was linearized in the equilibrium point $x = \begin{bmatrix} 0 & 0 & 0 & 0 & 0 & 0 & 0 \end{bmatrix}^\top$. The linear model has the form

$$\dot{x} = Ax + Bu. \tag{22}$$

After substituting the values of Table I,

$$A = \begin{bmatrix} -13.1706 & 0 & 0 & \dots \\ 0 & -13.1532 & -128.3055 & \dots \\ 0 & 0 & 0 & \dots \\ 0 & 6.2508 & 84.7584 & \dots \\ 0 & 0 & 0 & \dots \\ 6.2623 & 0 & 0 & \dots \\ 0 & 0 & 0 & \dots \end{bmatrix}$$

$$\begin{bmatrix} \dots & 0 & -128.5417 & 0 & 0 \\ \dots & 0 & 0 & 0 & 0 \\ \dots & 1 & 0 & 0 & 0 \\ \dots & 0 & 0 & 0 & 0 \\ \dots & 0 & 0 & 1 & 0 \\ \dots & 0 & 84.9145 & 0 & 0 \\ \dots & 0 & 0 & 0 & 0 \end{bmatrix}, \quad (23)$$

and

$$B = \begin{bmatrix} -39.8656 & 19.9328 & 19.9328 \\ 0 & -34.4790 & 34.4790 \\ 0 & 0 & 0 \\ 0 & 16.3855 & -16.3855 \\ 0 & 0 & 0 \\ 18.9552 & -9.4776 & -9.4776 \\ -30.9915 & -30.9915 & -30.9915 \end{bmatrix}. \quad (24)$$

IV. Control Design

The Linear Quadratic Regulator consists of a state feedback and was implemented only to regulate the system, that is, to keep the states at zero. The control law is given by

$$u = -Kx. \quad (25)$$

where K is defined in order to minimize the functional

$$J = \int_0^\infty \left(x^\intercal(t)Qx(t) + u^\intercal(t)Ru(t)\right)\, dt, \quad (26)$$

being Q and R semi-definite positive and definite positive matrices, respectively. These matrices are used to weight the influence of the states and inputs in the control.

The matrices Q and R were determined using the Bryson rule, seeking to normalize the effect of states and inputs on the functional (26), such that

$$Q_{ii} = \frac{1}{x_{i,\max}^2} \quad (27)$$

and

$$R_{jj} = \frac{1}{u_{j,\max}^2}, \quad (28)$$

where $x_{i,\max}$ is the maximum accepted variance for state i and $u_{j,\max}$ is the maximum value of input j. The maximum values chosen for each state variable are:

$$\begin{cases} \dot{\theta}x, \max &= 1.5 \text{ rad/s} \\ \dot{\theta}_y, \max &= 1.5 \text{ rad/s} \\ \theta_p, \max &= 10\pi/180 \text{ rad} \\ \dot{\theta}_p, \max &= 30\pi/180 \text{ rad/s} \\ \theta_r, \max &= 10\pi/180 \text{ rad} \\ \dot{\theta}_r, \max &= 30\pi/180 \text{ rad/s} \\ \dot{\theta}_w, \max &= 30\pi/180 \text{ rad/s} \end{cases}$$

The maximum value for the PWM signal was 100%, that is, 1. This resulted in a R matrix equal to a 3×3 identity (I_3). However, observing the experiments, it was noted the need to penalize the control input. At the end of the tests, it was adopted $R = 400I_3$.

The resulting control gain matrix is given by

$$K = \begin{bmatrix} 0.4691 & 0 & 0 & 0 & \cdots \\ -0.2346 & 0.4063 & 8.1251 & 1.2439 & \cdots \\ -0.2346 & -0.4064 & -8.1251 & -1.2439 & \cdots \end{bmatrix}$$
$$\begin{bmatrix} 9.3800 & 1.4352 & -0.0537 \\ -4.6900 & -0.7176 & -0.0537 \\ -4.6900 & -0.7176 & -0.0537 \end{bmatrix} \quad (29)$$

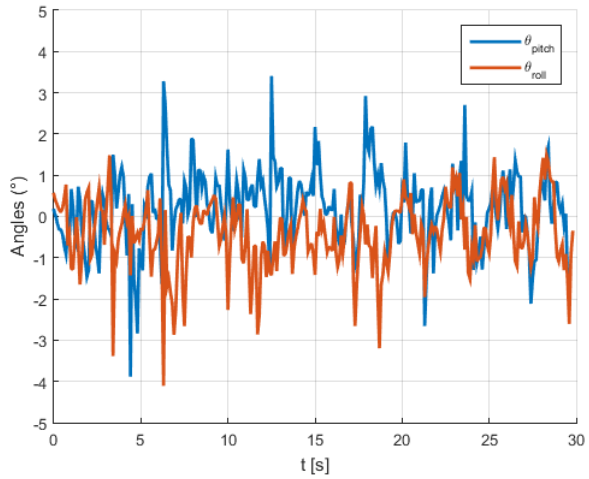

Fig. 6. Results of angular positions of the body.

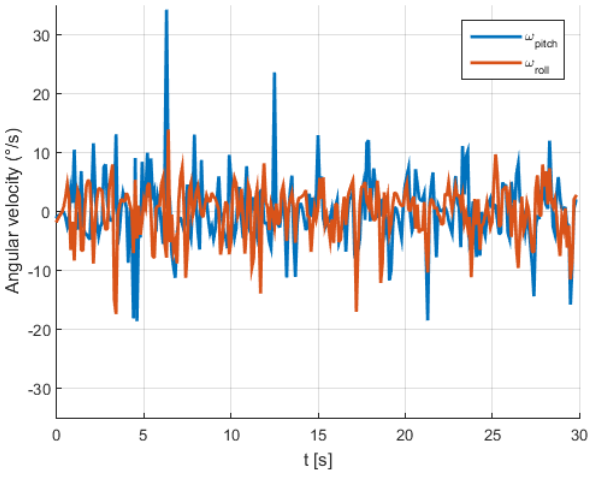

Fig. 7. Results of angular velocities of the body.

V. Practical Results

The practical results were obtained considering an experiment with duration of 30 seconds. The angular positions of the body are represented in Fig. 6

As can be observed, the controller was able to keep the body angles within the range $-4°$ and $4°$. In this range, it is valid to consider the linearized model as a good approximation to represent the behavior of the system. In Fig. 7, the results for the angular velocities of the body are presented

It is possible to observe that, in general, the pitch and roll velocities have remained within the error range projected in the LQR, i.e., below $30°/s$. Fig. 8 presents the control efforts in percentage of PWM duty cycle. Negative signal means reversing direction.

It is possible to observe that the control efforts did not exceed the range of 50% of its capacity during the test.

VI. Conclusions

The BBR was successfully built, modeled and controlled. The proposed modeling was good enough to design a model-based regulator. With the designed LQR, it was possible

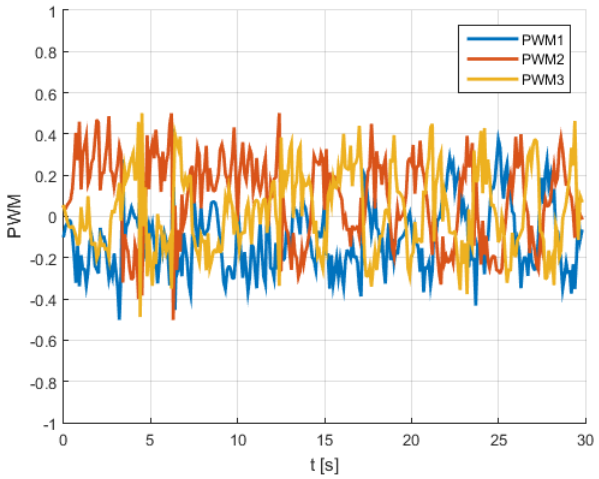

Fig. 8. Results of control efforts.

to balance the BBR within a range of $\pm 4^{\circ}$. However, for moderate to high impulsive disturbances and surfaces with significant irregularities (for instance, holes), the robot was not able to recover the equilibrium. However, this can be improved with a more powerful actuator. As suggestions of future work, it is possible to change the actuators to more powerful ones, to design robust and non-linear controllers, as well as to couple a computer vision system for the system to be able to follow a trajectory and to avoid obstacles.

REFERENCES

[1] T. B. Lauwers, G. A. Kantor, and R. L. Hollis, "A dynamically stable single-wheeled mobile robot with inverse mouse-ball drive," in *Proceedings 2006 IEEE International Conference on Robotics and Automation (ICRA 2006)*, May 2006, pp. 2884–2889.

[2] M. Kumagai and T. Ochiai, "Development of a robot balancing on a ball," in *2008 International Conference on Control, Automation and Systems*, Oct 2008, pp. 433–438.

[3] U. Nagarajan, A. Mampetta, G. A. Kantor, and R. Hollis, "State transition, balancing, station keeping and yaw control for a dynamically stable single spherical wheel mobile robot," in *Proceedings of the IEEE International Conference on Robotics & Automation (ICRA 2009)*, May 2009, pp. 998 – 1003.

[4] M. Kumagai and T. Ochiai, "Development of a robot balancing on a ball," in *2008 International Conference on Control, Automation and Systems*, Oct 2008, pp. 433–438.

[5] D. B. Pham, H. Kim, J. Kim, and S. G. Lee, "Balancing and transferring control of a ball segway using a double-loop approach [applications of control]," *IEEE Control Systems*, vol. 38, no. 2, pp. 15–37, April 2018.

[6] S. I. Han and J. M. Lee, "Balancing and velocity control of a unicycle robot based on the dynamic model," *IEEE Transactions on Industrial Electronics*, vol. 62, no. 1, pp. 405–413, Jan 2015.

[7] K. van der Blonk, "Modeling and control of a ball-balancing robot," Master's thesis, Internship & Master thesis at ALTEN Mechatronics, Eindhoven, 2014.